

Reactions of Titanium Dioxides with Acetylene Molecules. A Matrix Isolation FTIR and Density Functional Study

Lei Miao, Jian Dong, Liang Yu, and Mingfei Zhou*

Shanghai Key Laboratory of Molecular Catalysts and Innovative Materials, Department of Chemistry & Laser Chemistry Institute, Fudan University, Shanghai 200433, P. R. China

Received: November 21, 2002; In Final Form: January 14, 2003

Reactions of titanium dioxide with acetylene molecules have been studied using matrix isolation infrared absorption spectroscopy. The titanium dioxide molecules were prepared by the reactions of laser-ablated titanium atoms with dioxygen. In solid argon, titanium dioxide molecule reacted with acetylene to form the $\text{TiO}_2\text{-C}_2\text{H}_2$ complex spontaneously on annealing. The complex underwent photochemical rearrangement to the OTi(OH)CCH and $\text{H}_2\text{Ti(CO)}_2$ isomers upon UV–visible photolysis. The product absorptions were identified by isotopic substitutions and density functional calculations of isotopic frequencies.

Introduction

The reactions of transition metal centers with small molecules are important for the understanding of the elemental reaction mechanisms of catalysis, surface chemistry, and so on. The chemical reactivity of bare neutral transition metal atoms as well as cations with hydrocarbons such as small alkanes and alkenes has been extensively studied.^{1–3} By contrast, the reactions of transition metal oxides, particularly neutral oxide molecules with small hydrocarbons are relatively less studied, in part because of the experimental difficulty in making “pure” transition metal oxide molecules for reaction studies.

Recent investigations in our laboratory have shown that laser-ablation combined with matrix isolation is a suitable technique in producing metal dioxide molecules for reaction study.^{4–8} As has been mentioned, the primary products from codeposition of some laser-ablated metal atoms with oxygen in excess argon are predominantly metal dioxide molecules. Hence, the reactions of the primary formed metal dioxide molecules with other small molecules doped in the reagent gas have been reported.^{4–8} In this paper, we report a study of reactions of titanium dioxide with acetylene molecules. We will show that the titanium dioxide molecule forms a stable complex with acetylene spontaneously in solid argon. The complex undergoes photon-induced rearrangement to form the OTi(OH)CCH and $\text{H}_2\text{Ti(CO)}_2$ molecules.

Titanium dioxide is an important compound that is frequently used as industrial catalysts and catalyst supports. It has been widely used as a catalyst in processes such as oligomerization and hydrogenation of acetylene and its derivatives.⁹ The acetylene and titanium dioxide reaction study is a simple system that can serve as a model for understanding the reactions of transition metal oxides with other more complicated organic substrates.

Experimental and Computational Methods

The experimental setup for pulsed laser ablation and matrix isolation FTIR spectroscopic investigation has been described in detail previously.¹⁰ Briefly, the 1064 nm fundamental of a

Nd:YAG laser (20 Hz repetition rate and 8 ns pulse width) was focused onto a rotating titanium metal target through a hole in a CsI window. The laser-ablated metal atoms were codeposited with oxygen and acetylene mixtures in excess argon onto the 11 K CsI window for 1 h at a rate of 3–5 mmol/h. C_2H_2 was subjected to several freeze–pump–thaw cycles before use. O_2 (Shanghai BOC, 99.6%), $^{13}\text{C}_2\text{H}_2$ and C_2D_2 (99%, Cambridge Isotope Laboratories), and $^{18}\text{O}_2$ (Isotec Inc., >97%) were used without further purification. Infrared spectra were recorded on a Bruker IFS 113V spectrometer at 0.5 cm^{-1} resolution using a DTGS detector. Matrix samples were annealed at different temperatures, and selected samples were subjected to broadband photolysis using a high-pressure mercury arc lamp.

Density functional theoretical calculations were performed using the Gaussian 98 program.¹¹ The Becke three parameter hybrid functional with the Lee–Yang–Parr correlation corrections (B3LYP) was used.^{12,13} The 6-311++G** basis set was used for H, C, and O atoms. The all electron basis set of Wachters–Hay as modified by Gaussian was used for Ti atom.^{14–16} Geometries were fully optimized and vibrational frequencies calculated with analytical second derivatives, and zero point vibrational energies were derived.

Results and Discussion

Matrix isolated titanium dioxide molecules were prepared by reactions of laser-ablated titanium atoms with molecule oxygen in excess argon. The reaction products from codeposition of laser-ablated titanium atoms with oxygen in excess argon have been previously studied by Andrews and co-workers.¹⁷ Here we first repeated the titanium atom and oxygen reaction experiments, but with relatively low laser energy, typically, 5–10 mJ/pulse. With this controlled laser energy, we managed to generate enough titanium metal atoms for reaction and also to minimize the possibility for the formation of multi-metal species. Sample deposition at 11 K revealed strong TiO_2 (946.8 and 917.0 cm^{-1})¹⁷ and O_4^- absorptions (953.8 cm^{-1}).¹⁸ Sample annealing to 25 K decreased the O_4^- absorptions and increased the TiO_2 absorptions. Subsequent 20 min broadband photolysis destroyed the O_4^- absorption and increased the TiO_2 absorptions.

New product absorptions were observed in the experiments with $\text{C}_2\text{H}_2/\text{O}_2$ mixture in excess argon as reagent gas. Figures

* Corresponding author. E-mail: mzhou@fudan.edu.cn.

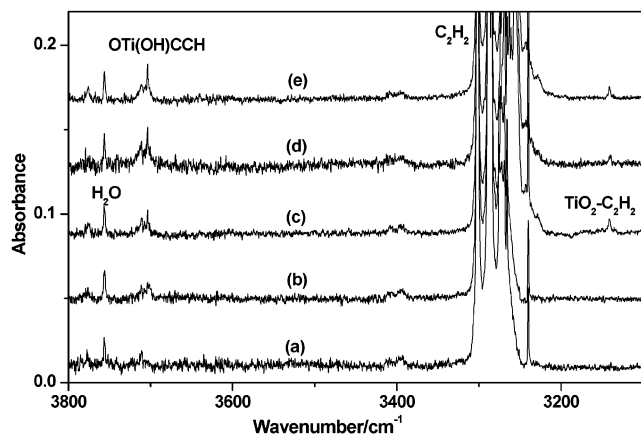


Figure 1. Infrared spectra in the 3800–3100 cm^{-1} region from codeposition of laser-ablated titanium atoms with 0.3% C_2H_2 + 0.6% O_2 in argon: (a) 1 h sample deposition at 11 K; (b) 20 min broadband photolysis; (c) 25 K annealing; (d) 20 min broadband photolysis; (e) 28 K annealing.

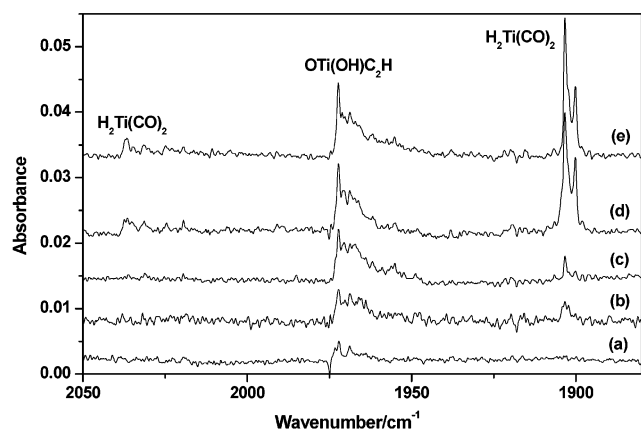


Figure 2. Infrared spectra in the 2050–1880 cm^{-1} region from codeposition of laser-ablated titanium atoms with 0.3% C_2H_2 + 0.6% O_2 in argon: (a) 1 h sample deposition at 11 K; (b) 20 min broadband photolysis; (c) 25 K annealing; (d) 20 min broadband photolysis; (e) 28 K annealing.

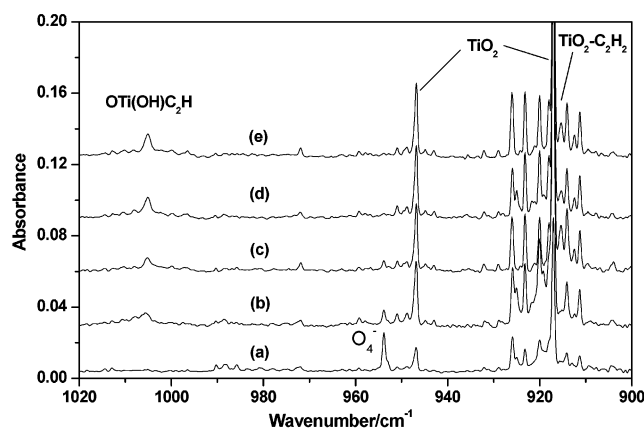


Figure 3. Infrared spectra in the 1020–900 cm^{-1} region from codeposition of laser-ablated titanium atoms with 0.3% C_2H_2 + 0.6% O_2 in argon: (a) 1 h sample deposition at 11 K; (b) 20 min broadband photolysis; (c) 25 K annealing; (d) 20 min broadband photolysis; (e) 28 K annealing.

1–3 show the spectra in the 3800–3100, 2050–1880, and 1020–900 cm^{-1} regions from codeposition of laser-ablated titanium atoms with 0.3% C_2H_2 and 0.6% O_2 in argon, and the product absorptions are listed in Table 1. Besides the titanium

TABLE 1: Infrared Absorptions (cm^{-1}) from Codeposition of Laser-Ablated Titanium Atoms and $\text{C}_2\text{H}_2/\text{O}_2$ Mixtures in Excess Argon

$\text{C}_2\text{H}_2/\text{O}_2$	$^{13}\text{C}_2\text{H}_2/\text{O}_2$	$\text{C}_2\text{H}_2/^{18}\text{O}_2$	$\text{C}_2\text{D}_2/\text{O}_2$	assignment
3703.5	3703.5	3692.1	2731.5	OTi(OH)CCH
3141.3	3127.8	3141.3	2364.5	$\text{TiO}_2\text{-C}_2\text{H}_2$
2036.6	1987.1	1990.1	2035.2	$\text{H}_2\text{Ti(CO)}_2$
1972.2	1904.0	1972.2	1859.0	OTi(OH)CCH
1903.3	1861.7	1857.9	1903.3	$\text{H}_2\text{Ti(CO)}_2$
1005.1	1005.0	963.0	1004.8	OTi(OH)CCH
946.8	946.8	904.3	946.8	$^{48}\text{TiO}_2$
917.0	917.0	881.6	881.6	$^{48}\text{TiO}_2$
915.4	915.4	880.3	912.5	$\text{TiO}_2\text{-C}_2\text{H}_2$

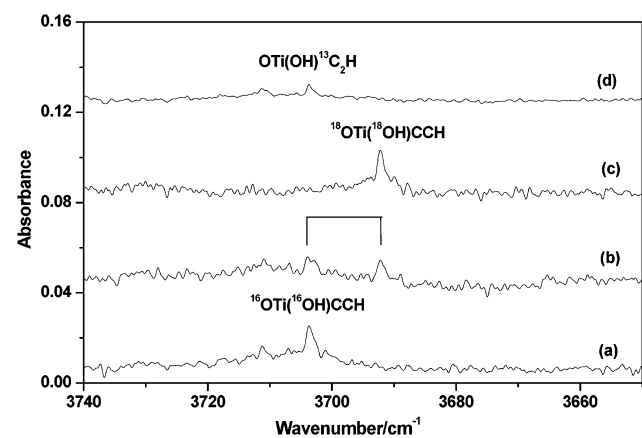


Figure 4. Infrared spectra in the 3740–3650 cm^{-1} region from codeposition of laser-ablated titanium atoms with $\text{C}_2\text{H}_2/\text{O}_2$ mixtures in excess argon: (a) 0.3% C_2H_2 + 0.6% O_2 ; (b) 0.3% C_2H_2 + 0.2% $^{16}\text{O}_2$ + 0.4% $^{16}\text{O}^{18}\text{O}$ + 0.2% $^{18}\text{O}_2$; (c) 0.3% C_2H_2 + 0.6% $^{18}\text{O}_2$; (d) 0.3% $^{13}\text{C}_2\text{H}_2$ + 0.8% O_2 .

oxide and oxygen cluster absorptions that are common to titanium and oxygen reactions, new product absorptions at 3141.3 and 915.4 cm^{-1} appeared together on 25 K annealing. These two new absorptions markedly decreased on broadband photolysis, when several new absorptions at 3703.5, 2036.6, 1972.2, 1903.3, and 1005.1 cm^{-1} were produced. The 3141.3 and 915.4 cm^{-1} bands were almost recovered, whereas the 3703.5, 2036.6, 1972.2, 1903.3, and 1005.1 cm^{-1} absorptions remained unchanged on subsequent 28 K annealing.

The experiments were repeated with $\text{C}_2\text{H}_2/^{18}\text{O}_2$, $\text{C}_2\text{H}_2/^{16}\text{O}_2$ + $^{16}\text{O}^{18}\text{O}$ + $^{18}\text{O}_2$, $^{13}\text{C}_2\text{H}_2/\text{O}_2$, $\text{C}_2\text{D}_2/\text{O}_2$ and $^{12}\text{C}_2\text{H}_2$ + $^{13}\text{C}_2\text{H}_2/\text{O}_2$ samples. The isotopic shifts and splittings of the new product absorptions are also listed in Table 1 and will be discussed in detail below. Representative spectra in selected regions using different isotopic samples are shown in Figures 4–6, respectively.

Calculation Results. To support the experimental assignments and to provide insight into the structure and bonding of the observed reaction products, we have performed density functional calculations, which can provide very reliable predictions of the state energies, structures and vibrational frequencies of transition metal-containing compounds.^{19–21} As a reference point, we calculated the TiCH molecule, which has been experimentally studied.²² The Ti–C and C–H bond lengths of $^2\Sigma^+$ ground-state TiCH were predicted to be 1.688 and 1.093 Å, compared to the experimental values of 1.728 and 1.085 Å. The Ti–C stretching and TiCH bending vibrational frequencies were observed at 855 and 578 cm^{-1} , whereas DFT calculation gave values of 947.8 and 604.2 cm^{-1} .

The calculated ground-state geometric parameters of the observed product molecules are shown in Figure 7, and the vibrational frequencies and intensities are listed in Table 2.

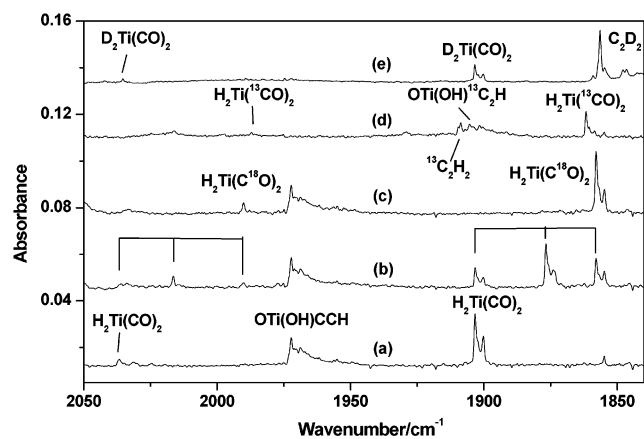


Figure 5. Infrared spectra in the 2050–1850 cm^{-1} region from codeposition of laser-ablated titanium atoms with $\text{C}_2\text{H}_2/\text{O}_2$ mixtures in excess argon: (a) 0.3% C_2H_2 + 0.6% O_2 ; (b) 0.3% C_2H_2 + 0.2% $^{16}\text{O}_2$ + 0.4% $^{16}\text{O}^{18}\text{O}$ + 0.2% $^{18}\text{O}_2$; (c) 0.3% C_2H_2 + 0.6% $^{18}\text{O}_2$; (d) 0.3% $^{13}\text{C}_2\text{H}_2$ + 0.8% O_2 ; (e) 0.3% C_2D_2 + 0.8% O_2 .

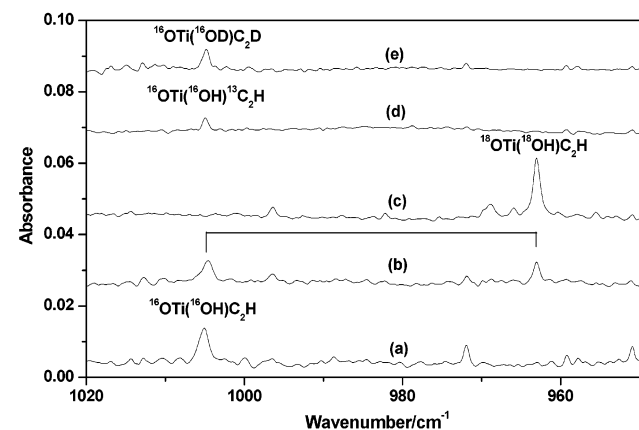


Figure 6. Infrared spectra in the 1020–950 cm^{-1} region from codeposition of laser-ablated titanium atoms with $\text{C}_2\text{H}_2/\text{O}_2$ mixtures in excess argon: (a) 0.3% C_2H_2 + 0.6% O_2 ; (b) 0.3% C_2H_2 + 0.2% $^{16}\text{O}_2$ + 0.4% $^{16}\text{O}^{18}\text{O}$ + 0.2% $^{18}\text{O}_2$; (c) 0.3% C_2H_2 + 0.6% $^{18}\text{O}_2$; (d) 0.3% $^{13}\text{C}_2\text{H}_2$ + 0.8% O_2 ; (e) 0.3% C_2D_2 + 0.8% O_2 .

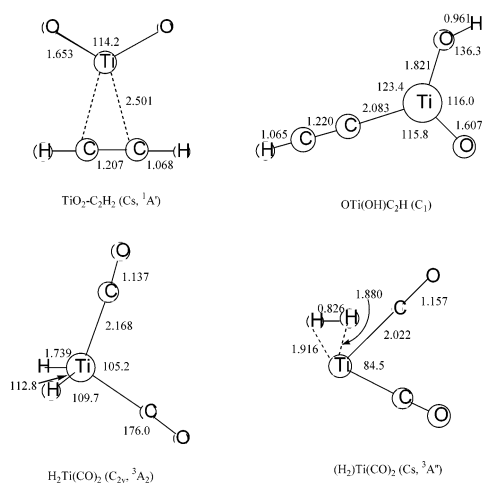


Figure 7. Calculated structures for different $\text{TiO}_2\text{C}_2\text{H}_2$ isomers (bond length in ångströms, bond angle in degrees).

$\text{TiO}_2\text{-C}_2\text{H}_2$. The absorptions at 915.4 and 3141.3 cm^{-1} are assigned to the $\text{TiO}_2\text{-C}_2\text{H}_2$ complex. These two absorptions increased together on annealing and decreased on photolysis. The 915.4 cm^{-1} band showed no carbon-13 isotopic shift with $\text{O}_2/^{13}\text{C}_2\text{H}_2$ and exhibited a very small (2.9 cm^{-1}) deuterium

TABLE 2: Calculated Vibrational Frequencies (cm^{-1}) and Intensities (in Parentheses, km/mol) for Different $\text{TiO}_2\text{C}_2\text{H}_2$ Isomers^a

$\text{TiO}_2\text{-C}_2\text{H}_2$ ($^1\text{A}'$)	OTi(OH)CCH	$\text{H}_2\text{Ti(CO)}_2$ ($^3\text{A}_2$)	$(\eta^2\text{-H}_2)\text{Ti(CO)}_2$ ($^3\text{A}'$)
3467.9 (12, a')	3894.9 (209)	2128.9 (396, a ₁)	3008.1 (1071, a'')
3376.4 (176, a'')	3444.2 (25)	2031.8 (2900, b ₂)	1979.9 (1229, a')
2015.7 (2, a')	2045.0 (119)	1641.2 (594, a ₁)	1929.7 (1567, a'')
1001.2 (46, a')	1065.9 (289)	1613.9 (601, b ₁)	1449.9 (51, a')
956.9 (388, a'')	754.0 (237)	547.3 (72, a ₁)	791.1 (182, a')
804.9 (91, a')	748.3 (39)	417.6 (63, b ₂)	545.7 (44, a')
757.7 (65, a')	699.2 (44)	372.7 (18, a ₁)	490.5 (0, a'')
703.0 (1, a'')	544.3 (171)	346.9 (0, a ₂)	435.4 (0, a'')
643.2 (0, a'')	516.5 (143)	332.6 (14, b ₁)	428.9 (4, a')
336.4 (15, a')	452.8 (90)	297.8 (1, a ₁)	411.0 (12, a')
261.0 (5, a'')	257.9 (19)	271.3 (17, b ₂)	407.8 (11, a'')
236.7 (19, a')	216.4 (4)	205.8 (0, a ₂)	346.8 (11, a')
128.7 (1, a'')	148.9 (52)	177.4 (416, b ₂)	272.8 (4, a')
104.7 (79, a')	98.0 (5)	144.4 (52, b ₁)	242.3 (4, a'')
20.3 (1, a'')	62.2 (24)	55.7 (0, a ₁)	73.9 (1, a')

^a The vibrational frequencies of ground state ($^1\text{A}_1$) TiO_2 were calculated at 1026.1 cm^{-1} (39 km/mol , a₁), 978.9 cm^{-1} (470 km/mol , b₂), and 339.7 cm^{-1} (15 km/mol , a₁). The vibrational frequencies of C_2H_2 were calculated at 3522.8 cm^{-1} (0 km/mol , σ_g), 3420.2 cm^{-1} (94 km/mol , σ_u), 2061.9 cm^{-1} (0, σ_g), 773.0 cm^{-1} (222 km/mol , π_u), and 661.2 cm^{-1} (0 km/mol , π_g).

isotopic shift with $\text{O}_2/\text{C}_2\text{D}_2$. This band shifted to 880.3 cm^{-1} when the $^{18}\text{O}_2/\text{C}_2\text{H}_2$ sample was used. The band position and the isotopic $^{16}\text{O}/^{18}\text{O}$ ratio of 1.0399 are very close to those of the antisymmetric stretching vibration of the TiO_2 molecule in solid argon (1.0401).¹⁷ This indicates that the 915.4 cm^{-1} band is due to an antisymmetric TiO_2 stretching vibration. Due to band overlap with the strong TiO_2 absorptions, the titanium isotopic splitting could not be observed for the 915.4 cm^{-1} band. The 3141.3 cm^{-1} band showed no oxygen-18 shift but was shifted to 3127.8 and 2364.5 cm^{-1} with $^{13}\text{C}_2\text{H}_2$ and C_2D_2 . The isotopic $^{12}\text{C}_2\text{H}_2/^{13}\text{C}_2\text{H}_2$ ratio of 1.0043 and H/D ratio of 1.3285 are indicative of a C–H stretching vibration.

Our DFT calculations on $\text{TiO}_2\text{-C}_2\text{H}_2$ predicted that the molecules have a singlet ground state ($^1\text{A}'$) with a nonplanar C_s symmetry. As can be seen in Table 2, the antisymmetric TiO_2 and C–H stretching vibrational frequencies were computed at 956.9 and 3376.4 cm^{-1} with 388/176 km/mol relative intensities. These two modes were predicted to be the most intense IR absorptions of the $\text{TiO}_2\text{-C}_2\text{H}_2$ complex. The calculated isotopic frequency ratios (Table 3) agree well with the experimental values. The $^1\text{A}'$ ground-state $\text{TiO}_2\text{-C}_2\text{H}_2$ complex can be viewed as the interaction of the closed-shell $^1\text{A}_1$ ground-state TiO_2 fragment and a slightly bent C_2H_2 fragment. Compared to free acetylene, the C–C and C–H bond lengths increase by only about 0.009 and 0.005 Å, and the C–H bonds move out of the CC axis and away from the Ti atom by only about 3.5°. The small deformation of the C_2H_2 ligand and the rather long Ti–C distances (2.501 Å) indicate weak interaction between the TiO_2 and C_2H_2 fragments. The bonding between TiO_2 and C_2H_2 fragments is mainly due to donation and back-donation mechanism. Theoretical calculations predicted that titanium dioxide can form a stable complex with water molecule,²³ but this complex was not observed in the reactions of titanium dioxide with water in solid argon.⁶

OTi(OH)CCH . The absorptions at 3703.5, 1972.2, and 1005.1 cm^{-1} maintained the same relative intensities throughout all the experiments, suggesting that they be due to different vibrational modes of the same species. The 3703.5 cm^{-1} band lies in the region expected for an O–H stretching vibration. This band showed no carbon-13 isotopic shift with $\text{O}_2/^{13}\text{C}_2\text{H}_2$ but shifted to 3692.1 cm^{-1} with $^{18}\text{O}_2/\text{C}_2\text{H}_2$, and to 2731.5 cm^{-1} with $\text{O}_2/\text{C}_2\text{D}_2$. The isotopic $^{16}\text{O}/^{18}\text{O}$ ratio of 1.0031 and H/D

TABLE 3: Comparison between Observed and Calculated Isotopic Frequency Ratios for the $\text{TiO}_2\text{-C}_2\text{H}_2$, OTi(OH)CCH , and $\text{H}_2\text{Ti(CO)}_2$ Molecules

cal	obs	$^{12}\text{C}/^{13}\text{C}$	$^{16}\text{O}/^{18}\text{O}$	H/D	$^{12}\text{C}/^{13}\text{C}$	$^{16}\text{O}/^{18}\text{O}$	H/D
$\text{H}_2\text{Ti(CO)}_2$	sym C–O str	1.0229	1.0241	1.0011	1.0249	1.0234	1.0007
	asym C–O str	1.0222	1.0256	1.0000	1.0223	1.0244	1.0000
$\text{TiO}_2\text{-C}_2\text{H}_2$	asym C–H str	1.0030	1.0000	1.3621	1.0043	1.0000	1.3285
	asym TiO_2 str	1.0000	1.0401	1.0005	1.0000	1.0399	1.0032
OTi(OH)CCH	O–H str	1.0000	1.0033	1.3728	1.0000	1.0031	1.3558
	C–C str	1.0373	1.0000	1.0678	1.0358	1.0000	1.0609
	Ti–O str	1.0000	1.0435	1.0000	1.0001	1.0437	1.0003

ratio of 1.3558 indicate that this band is due to an O–H stretching vibration. In the mixed $^{16}\text{O}_2 + ^{16}\text{O}^{18}\text{O} + ^{18}\text{O}_2/\text{C}_2\text{H}_2$ experiment, only the pure isotopic counterparts were observed, indicating that only one OH is involved in this mode. The 1972.2 cm^{-1} band exhibited no oxygen-18 shift but shifted to 1904.0 cm^{-1} with $\text{O}_2/^{13}\text{C}_2\text{H}_2$. The isotopic $^{12}\text{C}/^{13}\text{C}$ ratio of 1.0358 is only slightly smaller than that of a pure C–C stretching vibration (1.0408). The 1972.2 cm^{-1} band should thus be assigned to a C–C stretching vibration mixing with some other vibrational components. The C_2D_2 counterpart was observed at 1858.0 cm^{-1} and gave an H/D ratio of 1.0609. The IR inactive but Raman active C–C stretching vibration of acetylene was observed at 1973.8 cm^{-1} with the C_2D_2 counterpart at 1762.4 cm^{-1} .²⁴ Note that the deuterium isotopic shift of acetylene (H/D ratio:1.1200) is about twice as large as the shift observed here for the 1972.2 cm^{-1} band. This suggests that there is less hydrogen involvement in the 1972.2 cm^{-1} mode than that in free acetylene, so only one hydrogen atom is most likely involved. These data point to the involvement of a CCH subunit in the molecule. In the reactions of transition metal atoms and acetylene, the ethynyliron hydride HFeCCH and ethynylchromium hydride HCrCCH molecules have been observed in solid argon matrix.^{24,25} The C–C stretching mode of HFeCCH and HCrCCH were observed at 1976.4 and 1955.2 cm^{-1} , respectively. The 1005.1 cm^{-1} band shifted to 963.0 cm^{-1} with $^{18}\text{O}_2/\text{C}_2\text{H}_2$ and gave an isotopic $^{16}\text{O}/^{18}\text{O}$ ratio of 1.0437. This ratio is slightly lower than the diatomic TiO ratio of 1.0446 in solid argon.¹⁷ The band position and isotopic ratio are very close to that of OTi(OH)_2 (996.6 cm^{-1} , 1.0430)⁶ and H_2TiO (1010.5 cm^{-1} , 1.0430).²⁶ These imply that the 1005.1 cm^{-1} band is due to a terminal Ti–O stretching vibration. The very small carbon-13 (0.1 cm^{-1}) and deuterium (0.3 cm^{-1}) shifts indicate that the coupling with C and H atoms is very small in this mode. The production of the 3703.5, 1972.2, and 1005.1 cm^{-1} bands at the expense of the $\text{TiO}_2\text{-C}_2\text{H}_2$ complex absorptions on photolysis suggest that these three bands be due to another structural isomer or photolysis fragment of the $\text{TiO}_2\text{-C}_2\text{H}_2$ complex. Accordingly, we assigned the 3703.5, 1972.2, and 1005.1 cm^{-1} bands to the O–H, C–C, and Ti–O stretching vibrations of the OTi(OH)CCH molecule.

The assignment was strongly supported by DFT calculations. The B3LYP functional predicted a singlet ground state for OTi(OH)CCH . The optimized structure is slightly nonplanar with C_1 symmetry (Figure 7). The calculated bond lengths are Ti–O = 1.607 Å, Ti–OH = 1.821 Å, Ti–C = 2.083 Å, and C–C = 1.220 Å. The TiCCH unit is almost linear. The Ti–C bond is a single bond, the bond length is slightly shorter than the standard Ti–C distances in tetraaryl compounds (2.13 Å).²⁷ The C–C bond is a triple bond, which is only slightly longer (0.021 Å) than that in the free acetylene calculated at the same level of theory.

The calculated frequencies at the optimized geometry of OTi(OH)CCH provided excellent support for the proposed identification of this molecule. As listed in Table 2, the Ti=O, O–H, and C–C stretching modes were calculated at 1065.9, 3894.9, and 2045.0 cm^{-1} , respectively. All of these three modes were

calculated to be intense with 289:209:119 km/mol relative intensities. Table 3 summarizes the comparison of the experimental and theoretical isotopic frequency ratios. The overall agreement between calculated and observed isotopic frequency ratios is quite convincing.

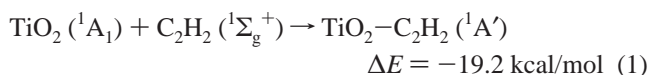
$\text{H}_2\text{Ti(CO)}_2$. The absorption at 1903.3 cm^{-1} increased markedly on broadband photolysis and almost remained unchanged on further annealing. This band exhibited no deuterium isotopic shift with $\text{C}_2\text{D}_2/\text{O}_2$ but shifted to 1861.7 cm^{-1} with $^{13}\text{C}_2\text{H}_2/\text{O}_2$ and to 1857.9 cm^{-1} with $\text{C}_2\text{H}_2/^{18}\text{O}_2$. The isotopic $^{12}\text{C}/^{13}\text{C}$ ratio of 1.0223 and $^{16}\text{O}/^{18}\text{O}$ ratio of 1.0244 are characteristic of a terminal C–O stretching vibration. When a 1:2:1 mixture of $^{16}\text{O}_2 + ^{16}\text{O}^{18}\text{O} + ^{18}\text{O}_2$ was used, the 1903.3 cm^{-1} band led to a triplet at 1903.3, 1876.8, and 1857.9 cm^{-1} with intensity ratios of approximately 1:2:1, indicating that two equivalent CO subunits are involved in this vibrational mode. A weak band at 2036.6 cm^{-1} exhibited the same annealing and photolysis behavior as the 1903.3 cm^{-1} band. The $^{13}\text{C}_2\text{H}_2/\text{O}_2$ and $\text{C}_2\text{H}_2/^{18}\text{O}_2$ substitutions shifted this band to 1987.1 and 1990.1 cm^{-1} , respectively. The isotopic $^{12}\text{C}/^{13}\text{C}$ ratio of 1.0249 and $^{16}\text{O}/^{18}\text{O}$ ratio of 1.0234 are appropriate for a carbonyl vibration. The mixed $\text{C}_2\text{H}_2/^{16}\text{O}_2 + ^{16}\text{O}^{18}\text{O} + ^{18}\text{O}_2$ experiment also reveals a triplet absorption with an intermediate at 2016.4 cm^{-1} . This mode has slightly more C and less O participation than the 1903.3 cm^{-1} mode. These data indicate that the 1903.3 and 2036.6 cm^{-1} bands are due to antisymmetric and symmetric C–O stretching vibrations of a bent Ti(CO)_2 unit. These frequencies are more than 100 cm^{-1} higher than that of the Ti(CO)_2 molecule, which was observed at 1799.3 and 1893.1 cm^{-1} in solid neon.²⁸ In the present experiments, no obvious associate absorption was observed, which makes the definitive assignment quite difficult. We note that the 2036.6 cm^{-1} band exhibited a small deuterium isotopic shift (1.4 cm^{-1}), denoting that this mode is slightly coupled by H atom(s). Therefore, the product contains one or more H atoms. Considering the fact that this molecule and the OTi(OH)CCH molecule were produced on photolysis at the expense of $\text{TiO}_2\text{-C}_2\text{H}_2$, its stoichiometric formula most likely should be $\text{H}_2\text{TiC}_2\text{O}_2$.

Extensive DFT calculations were performed to support the assignment. Two geometries were considered: a dihydrogen complex form ($(\eta^2\text{-H}_2)\text{Ti(CO)}_2$) and a dihydride form ($\text{H}_2\text{Ti(CO)}_2$). The ground state of the $(\eta^2\text{-H}_2)\text{Ti(CO)}_2$ complex was predicted to be a $^3\text{A}''$, followed by a $^5\text{A}_1$ state, which lies 3.6 kcal/mol above the $^3\text{A}''$ ground state. The $^3\text{A}''$ state ($\eta^2\text{-H}_2$)- Ti(CO)_2 has C_s symmetry, with a symmetry plane containing the $\text{Ti(H}_2)$ subunit. The $^5\text{A}_1$ state structure has a planar C_{2v} symmetry. We have also carried out geometry optimization for the singlet and triplet spin states of the $\text{H}_2\text{Ti(CO)}_2$ dihydride structure and found a $^3\text{A}_2$ state to be the most stable. The lowest singlet state of $\text{H}_2\text{Ti(CO)}_2$ ($^1\text{A}_1$) is only about 2.1 kcal/mol less stable than the $^3\text{A}_2$ state. Both the $^3\text{A}_2$ and $^1\text{A}_1$ state $\text{H}_2\text{Ti(CO)}_2$ structures have C_{2v} symmetry with the TiH_2 plane perpendicular to the Ti(CO)_2 plane. At the B3LYP/6-311++G(d, p) level of theory, the $^3\text{A}_2$ ground-state $\text{H}_2\text{Ti(CO)}_2$ dihydride form was predicted to be 5.1 kcal/mol lower in energy than the $^3\text{A}''$ state

$(\eta^2\text{-H}_2)\text{Ti}(\text{CO})_2$ dihydrogen complex form. The optimized geometric parameters for these structures are shown in Figure 7, and the vibrational frequencies and intensities are given in Table 2.

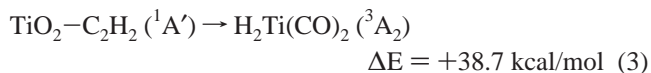
As listed in Table 2, the symmetric and antisymmetric C–O stretching vibrations for the $^3A''$ state $(\eta^2\text{-H}_2)\text{Ti}(\text{CO})_2$ dihydrogen complex were predicted at 1979.9 and 1929.7 cm^{-1} with 1229:1567 km/mol relative intensities. The symmetric mode is about 56 cm^{-1} lower than the observed frequency, and the predicted relative intensities are also inconsistent with the experimental observations. The H–H stretching mode was computed at 3008.1 cm^{-1} with comparable intensity (1071 km/mol). The two C–O stretching modes for the 3A_2 state $\text{H}_2\text{Ti}(\text{CO})_2$ dihydride were calculated at 2128.9 and 2031.8 cm^{-1} with 396:2900 km/mol relative intensities. The calculated frequencies are 4.5 and 6.8% higher than the experimental values. The DFT normal-mode analysis shows that the lower mode is a pure antisymmetric C–O stretching, and the upper mode is a symmetric C–O stretching slightly coupled with the H atoms (2.4 cm^{-1} deuterium shift), which are consistent with the experimentally observed isotopic effects on the frequencies. However, there is discrepancy between calculation and experiment. The symmetric and antisymmetric Ti–H stretching modes were predicted at 1641.2 and 1613.9 cm^{-1} with appreciable intensities (594 and 601 km/mol), but we were not able to observe these two bands. We suspect that DFT calculations overestimate the relative intensities of the Ti–H stretching modes. There are some examples where theoretical calculations do not provide very reliable IR intensity predictions. In a recent study on the reaction of titanium and ethylene, DFT calculations overestimated some absorptions such as C–H stretching of vinyltitanium hydride.²⁹ In our previous work on the reactions of CrO_2 and H_2 , the relative intensities of the H–H and Cr–H stretching vibrations of the reaction products were also underestimated by DFT calculations.⁵

Reaction Mechanism. The primary reaction product from codeposition of laser-ablated titanium atoms and $\text{O}_2/\text{C}_2\text{H}_2$ mixtures in excess argon is titanium dioxide. It is interesting to note that the TiO , Ti_2O_2 and O_3 absorptions were hardly observed in present low laser energy experiments, indicating that the yields of O atoms and other titanium oxide species are rather low. No titanium–acetylene reaction product was observed after sample deposition. These results indicate that the oxygen reaction is given preference over the acetylene reaction. Sample annealing allowed the acetylene molecules to diffuse in solid argon and to react with the primary reaction product: TiO_2 . Hence, the $\text{TiO}_2\text{-C}_2\text{H}_2$ absorptions were produced via reaction 1. This reaction was predicted to be exothermic by



about 19.2 kcal/mol after zero point energy corrections. The $\text{TiO}_2\text{-C}_2\text{H}_2$ complex absorptions increased on annealing, which suggests that reaction 1 requires negligible activation energy.

The $\text{OTi}(\text{OH})\text{CCH}$ and $\text{H}_2\text{Ti}(\text{CO})_2$ absorptions were produced on broadband photolysis when the $\text{TiO}_2\text{-C}_2\text{H}_2$ complex absorptions decreased, suggesting that the $\text{OTi}(\text{OH})\text{CCH}$ and $\text{H}_2\text{Ti}(\text{CO})_2$ molecules are formed by photochemical rearrangement of the $\text{TiO}_2\text{-C}_2\text{H}_2$ complex, reactions 2 and 3. Reaction 2 is a H atom transfer reaction. One H atom of the C_2H_2 unit in $\text{TiO}_2\text{-C}_2\text{H}_2$ is transferred to one of the O atoms in the TiO_2 unit to form the $\text{OTi}(\text{OH})\text{CCH}$ molecule. This H atom transfer process involves the breaking of one C–H σ bond and one Ti–O π bond, with the formation of one O–H bond and one Ti–C bond.



Similar H atom transfer reactions have been observed in various transition metal atom reaction systems^{2,25,26,29–31} as well as some dioxide reaction systems^{5–7} and have been shown to occur via a four-center transition state with a low energy barrier. Reaction 2 was predicted to be exothermic by about 33.0 kcal/mol at the B3LYP/6-311++G(d,p) level. As has been mentioned, both the $\text{TiO}_2\text{-C}_2\text{H}_2$ complex and the $\text{OTi}(\text{OH})\text{CCH}$ molecule have a singlet ground state; therefore, reaction 2 conserves spin.

Reaction 3 probably proceeds via a complicated process. This reaction is predicted to be endothermic by about 38.7 kcal/mol . As the $\text{H}_2\text{Ti}(\text{CO})_2$ molecule has a triplet ground state, reaction 3 involves spin crossing. It is interesting to note that the $\text{OTi}(\text{OH})\text{CCH}$ absorptions observed on $\lambda > 290 \text{ nm}$ photolysis, but the $\text{H}_2\text{Ti}(\text{OH})_2$ absorptions only appeared on full arc photolysis. This indicates that higher energy UV excitation is required to initiate rearrangement reaction 3 than reaction 2.

Conclusions

Laser-ablated titanium atoms codeposited with $\text{C}_2\text{H}_2/\text{O}_2$ mixtures in excess argon to form titanium dioxide as the primary product. Sample annealing allowed the C_2H_2 molecules to diffuse and react with the titanium dioxide molecules. Hence, the $\text{TiO}_2\text{-C}_2\text{H}_2$ complex was produced spontaneously on annealing. Broadband UV–visible photolysis destroyed the complex and produced two structural isomers: $\text{OTi}(\text{OH})\text{CCH}$ and $\text{H}_2\text{Ti}(\text{CO})_2$. These new product absorptions were identified by isotopic substitutions. The ground state, equilibrium structures and vibrational frequencies of these molecules have also been determined by density functional calculations.

Acknowledgment. We greatly acknowledge financial support from NSFC (20003003 and 20125033) and the NKBRSF of China.

References and Notes

- (1) Transition metal cation reactions, see, for example: van Koppen, P. A. M.; Bowers, M. T.; Haynes, C. L.; Armentrout, P. B. *J. Am. Chem. Soc.* **1998**, *120*, 5704. Eller, K.; Schwarz, H. *Chem. Rev.* **1991**, *91*, 1121. Armentrout, P. B.; Beauchamp, J. L. *Acc. Chem. Res.* **1989**, *22*, 315.
- (2) Transition metal atom reactions in the gas phase, see, for example: Carroll, J. J.; Haug, K. L.; Weisshaar, J. C.; Blomberg, M. R. A.; Siegbahn, P. E. M.; Svensson, M. *J. Phys. Chem.* **1995**, *99*, 13955. Ritter, D.; Carroll, J. J.; Weisshaar, J. C. *J. Phys. Chem.* **1992**, *96*, 10636. Carroll, J. J.; Weisshaar, J. C. *J. Phys. Chem.* **1996**, *100*, 12355.
- (3) Transition metal atom reactions in solid matrices, see, for example: Hauge, R. H.; Margrave, J. L. In *Chemistry and Physics of Matrix-Isolated Species*; Andrews, L., Moskovits, M., Eds.; North-Holland: New York, 1989.
- (4) Zhou, M. F.; Zhang, L. N.; Qin, Q. Z. *J. Phys. Chem. A* **2001**, *105*, 6407.
- (5) Zhou, M. F.; Zhang, L. N.; Shao, L. M.; Wang, W. N.; Fan, K. N.; Qin, Q. Z. *J. Phys. Chem. A* **2001**, *105*, 10747.
- (6) Shao, L. M.; Zhang, L. N.; Chen, M. H.; Lu, H.; Zhou, M. H. *Chem. Phys. Lett.* **2001**, *343*, 178.
- (7) Zhou, M. F.; Chen, M. H. *Chem. Phys. Lett.* **2001**, *349*, 64.
- (8) Miao, L.; Shao, L. M.; Wang, W. N.; Fan, K. N.; Zhou, M. F. *J. Chem. Phys.* **2002**, *116*, 5643.
- (9) See, for example: Sherrill, A. B.; Barteau, M. A. *J. Mol. Catal. A-Chem.* **2002**, *184*, 3011. Pierce, K. G.; Barteau, M. A. *J. Phys. Chem.* **1994**, *98*, 3882. Sakata, Y.; Lin, Z. H.; Imamura, H.; Tsuchiya, S. *J. Chem. Soc. Chem. Commun.* **1991**, *19*, 1392. Kang, J. H.; Shin, E. W.; Kim, W. J.; Park, J. D.; Moon, S. H. *J. Catal.* **2002**, *208*, 310.
- (10) Chen, M. H.; Wang, X. F.; Zhang, L. N.; Yu, M.; Qin, Q. Z. *Chem. Phys.* **1999**, *242*, 81. Zhou, M. F.; Zhang, L. N.; Qin, Q. Z. *J. Am. Chem. Soc.* **2000**, *122*, 4483.

- (11) Frisch, M. J.; Trucks, G. W.; Schlegel, H. B.; Scuseria, G. E.; Robb, M. A.; Cheeseman, J. R.; Zakrzewski, V. G.; Montgomery, J. A., Jr.; Stratmann, R. E.; Burant, J. C.; Dapprich, S.; Millam, J. M.; Daniels, A. D.; Kudin, K. N.; Strain, M. C.; Farkas, O.; Tomasi, J.; Barone, V.; Cossi, M.; Cammi, R.; Mennucci, B.; Pomelli, C.; Adamo, C.; Clifford, S.; Ochterski, J.; Petersson, G. A.; Ayala, P. Y.; Cui, Q.; Morokuma, K.; Malick, D. K.; Rabuck, A. D.; Raghavachari, K.; Foresman, J. B.; Cioslowski, J.; Ortiz, J. V.; Baboul, A. G.; Stefanov, B. B.; Liu, G.; Liashenko, A.; Piskorz, P.; Komaromi, I.; Gomperts, R.; Martin, R. L.; Fox, D. J.; Keith, T.; Al-Laham, M. A.; Peng, C. Y.; Nanayakkara, A.; Gonzalez, C.; Challacombe, M.; Gill, P. M. W.; Johnson, B.; Chen, W.; Wong, M. W.; Andres, J. L.; Gonzalez, C.; Head-Gordon, M.; Replogle, E. S.; Pople, J. A. *Gaussian 98*, Revision A.7; Gaussian, Inc.: Pittsburgh, PA, 1998.
- (12) Becke, A. D. *J. Chem. Phys.* **1993**, *98*, 5648.
- (13) Lee, C.; Yang, E.; Parr, R. G. *Phys. Rev. B* **1988**, *37*, 785.
- (14) McLean, A. D.; Chandler, G. S. *J. Chem. Phys.* **1980**, *72*, 5639.
- (15) Krishnan, R.; Binkley, J. S.; Seeger, R.; Pople, J. A. *J. Chem. Phys.* **1980**, *72*, 650.
- (16) Wachtters, A. J. H. *J. Chem. Phys.* **1970**, *52*, 1033. Hay, P. J. *J. Chem. Phys.* **1977**, *66*, 4377.
- (17) Chertihin, G. V.; Andrews, L. *J. Phys. Chem.* **1995**, *99*, 6356.
- (18) Zhou, M. F.; Hacıoğlu, J.; Andrews, L. *J. Chem. Phys.* **1999**, *110*, 9450. Jacox, M. E.; Thompson, W. E. *J. Chem. Phys.* **1994**, *100*, 750.
- (19) Bauschlicher, C. W., Jr.; Ricca, A.; Partridge, H.; Langhoff, S. R. In *Recent Advances in Density Functional Theory*; Chong, D. P., Ed.; World Scientific Publishing: Singapore, 1997; Part II.
- (20) Siegbahn, P. E. M. Electronic Structure Calculations for Molecules Containing Transition Metals. *Adv. Chem. Phys.* **1996**, XCIII.
- (21) Frenking, G.; Fröhlich, N. *Chem. Rev.* **2000**, *100*, 717.
- (22) Barnes, M.; Merer, A. J.; Metha, G. F. *J. Mol. Spectrosc.* **1997**, *181*, 168.
- (23) Johnson, J. R. T.; Panas, I. *Inorg. Chem.* **2000**, *39*, 3192.
- (24) Kline, E. S.; Kafafi, Z. H.; Hauge, R. H.; Margrave, J. L. *J. Am. Chem. Soc.* **1985**, *107*, 7559.
- (25) Huang, Z. G.; Zeng, A. H.; Dong, J.; Zhou, M. F. *J. Phys. Chem. A*, in press.
- (26) Zhou, M. F.; Zhang, L. N.; Dong, J.; Qin, Q. Z. *J. Am. Chem. Soc.* **2000**, *122*, 10680.
- (27) Bassi, I.; Allegra, G.; Scordamaglia, R.; Chiccola, G. *J. Am. Chem. Soc.* **1971**, *93*, 3787.
- (28) Zhou, M. F.; Andrews, L. *J. Phys. Chem. A* **1999**, *103*, 5259.
- (29) Lee, Y. K.; Manceron, L.; Papai, I. *J. Phys. Chem. A* **1997**, *101*, 9650.
- (30) Zhou, M. F.; Dong, J.; Zhang, L. N.; Qin, Q. Z. *J. Am. Chem. Soc.* **2001**, *123*, 135. Zhou, M. F.; Zhang, L. N.; Shao, L. M.; Wang, W. N.; Fan, K. N.; Qin, Q. Z. *J. Phys. Chem. A* **2001**, *105*, 5801. Zhang, L. N.; Zhou, M. F.; Shao, L. M.; Wang, W. N.; Fan, K. N.; Qin, Q. Z. *J. Phys. Chem. A* **2001**, *105*, 6998.
- (31) Zhou, M. F.; Chen, M. H.; Zhang, L. N.; Lu, H. *J. Phys. Chem. A* **2002**, *106*, 9017. Chen, M. H.; Lu, H.; Dong, J.; Miao, L.; Zhou, M. F. *J. Phys. Chem. A* **2002**, *106*, 11456. Chen, M. H.; Zeng, A. H.; Lu, H.; Zhou, M. F. *J. Phys. Chem. A* **2002**, *106*, 3077.